View angle dependence of cloud optical thicknesses retrieved by MODIS

Tamás Várnai
Joint Center for Earth System Technology, University of Maryland, Baltimore County

Alexander Marshak
Climate and Radiation Branch, NASA Goddard Space Flight Center

Prepared for the *Journal of Geophysical Research*
November, 2005

Popular Summary

Satellite remote sensing is such a complex task that until now it could be done only assuming that clouds are homogeneous slabs. This assumption does not consider that horizontal cloud variability may influence the amount of sunlight clouds reflect toward a satellite. This study examines whether horizontal cloud variability causes satellite estimates of cloud optical thickness to yield different results if clouds are viewed from different directions. The statistical analysis of water clouds (excluding ice-clouds for simplicity) in a one year long global dataset of observations by the Moderate Resolution Imaging Spectroradiometer (MODIS) reveals that while the estimated optical thickness values are consistent for all view directions if clouds are homogeneous, the values are much higher for oblique views than for overhead views if clouds are heterogeneous and the sun is fairly oblique. After considering a variety of possible scenarios, the paper concludes that the most likely reason for estimating larger optical thicknesses at oblique views is the enhanced viewing of cloud sides from oblique directions. The results will help understand the uncertainties cloud variability introduces into satellite estimations of optical thickness. They complement the uncertainty estimates that will start accompanying MODIS cloud products in the near future and may eventually help correct for the observed view angle dependent biases.

View angle dependence of cloud optical thicknesses retrieved by MODIS

Tamás Várnai
Joint Center for Earth System Technology,
University of Maryland, Baltimore County

Alexander Marshak
Climate and Radiation Branch
NASA Goddard Space Flight Center

Prepared for the *Journal of Geophysical Research*

November, 2005

Corresponding author address: Tamás Várnai, Code 613.2, NASA GSFC, Greenbelt, MD 20771, USA. Email: varnai@climate.gsfc.nasa.gov.

Abstract

This study examines whether cloud inhomogeneity influences the view angle dependence of MODIS cloud optical thickness (τ) retrieval results. The degree of cloud inhomogeneity is characterized through the local gradient in 11 μm brightness temperature. The analysis of liquid phase clouds in a one year long global dataset of Collection 4 MODIS data reveals that while optical thickness retrievals give remarkably consistent results for all view directions if clouds are homogeneous, they give much higher τ-values for oblique views than for overhead views if clouds are inhomogeneous and the sun is fairly oblique. For solar zenith angles larger than 55°, the mean optical thickness retrieved for the most inhomogeneous third of cloudy pixels is more than 30% higher for oblique views than for overhead views. After considering a variety of possible scenarios, the paper concludes that the most likely reason for the increase lies in three-dimensional radiative interactions that are not considered in current, one-dimensional retrieval algorithms. Namely, the radiative effect of cloud sides viewed at oblique angles seems to contribute most to the enhanced τ-values. The results presented here will help understand cloud retrieval uncertainties related to cloud inhomogeneity. They complement the uncertainty estimates that will start accompanying MODIS cloud products in Collection 5 and may eventually help correct for the observed view angle dependent biases.

Keywords: cloud, remote sensing, radiation, inhomogeneity

1. Introduction

Satellite remote sensing is such a complex task that until now it could be done only by using one-dimensional (1D) radiative transfer theory, which assumes that cloudy pixels are fully covered by horizontally homogeneous clouds and that the pixels' radiative properties are not affected by cloud variability in nearby areas. The use of 1D theory is often referred to as the plane-parallel approximation. It is true that some recently proposed methods (e.g., Marshak et al. 1998, Oreopoulos et al. 2000a, Faure et al. 2001, Várnai and Marshak 2002a, Iwabuchi and Hayasaka 2003, Cornet et al. 2004, 2005) use some aspects of three-dimensional (3D) radiative transfer theory for retrievals of cloud optical thickness, but these novel methods are not yet ready for operational use.

In recent years, several observational studies examined whether 1D radiative theory gives accurate results in satellite remote sensing. These studies found that, under certain conditions, 3D effects cause significant problems. Specifically, they revealed that 3D effects can make clouds appear too smooth (e.g., Marshak et al. 1995, Davis et al. 1997), too bright and thick (e.g., Loeb and Davies 1996, Loeb and Coakley 1998), and artificially asymmetric (Várnai and Marshak 2002a,b).

While the papers above focused mainly on overhead satellite views, some studies examined 3D effects for oblique views. A comparison of GOES and Meteosat radiances for scenes that were viewed from different directions by the two satellites did not reveal any influence of 3D effects (Rossow 1989). Using multiangle MISR (Multiangle Imaging SpectroRadiometer) observations, however, Horváth and Davies (2004) showed that the angular pattern of cloud reflection rarely fits the expectations based on the plane-parallel

approximation. Examining ERBE (Earth Radiation Budget Experiment), AVHRR (Advanced Very High-Resolution Radiometer), and POLDER (Polarization and Directionality of the Earth's Reflectances) data, some other studies (Loeb and Davies 1997; Loeb and Coakley 1998; Buriez et al. 2001) found that for low sun, 3D interactions such as shadowing make clouds appear too dark from oblique views facing the sun, and that this makes 1D retrievals underestimate cloud optical thickness. Theoretical studies (e.g., Davies 1984; Kobayashi 1993; Loeb et al. 1998; Szczap et al. 2000; Várnai 2000; Chambers et al. 2001; Iwabuchi and Hayasaka 2002) have long suggested that 3D effects have an opposite influence for oblique views facing away from the sun—but the observations cited above have not confirmed unambiguously the existence of this enhanced backscatter from sunlit slopes. Zuidema et al. (2003) found that in highly inhomogeneous cumulus congestus clouds, oblique backscatter reflectances observed by MISR exceeded 3D radiative transfer calculations based on cloud structure retrieved from the MISR nadir camera using the plane-parallel approximation. Recently, Marchand and Ackerman (2004) found that stratocumulus reflection in backscatter direction was stronger in MISR observations than in 1D or even 2D simulations based on a variety of ground-based and satellite observations.

Finally, theoretical studies (e.g., Davies 1984, Bréon 1992, Kobayashi 1993, Iwabuchi and Hayasaka 2002) also showed that cloud inhomogeneities can enhance reflection into oblique side scatter directions relative to reflection into nadir direction. The observations of Minnis (1989) revealed that cloud side viewing must occur frequently, because it increases cloud coverage significantly for oblique views. Still, while the viewing of cloud sides can be expected to yield larger retrieved optical

thicknesses for oblique side scatter views than for overhead views, the significance of this effect has not yet been determined through observations.

The goal of this paper is to analyze the view angle dependence of a one year long MODIS cloud optical thickness dataset, and to examine whether cloud inhomogeneity has a significant influence on this view angle dependence. Section 2 describes the data we analyzed, Section 3 outlines our methodology, and Section 4 presents the results of our analysis. Section 5 then discusses potential reasons for the observed view angle dependence, including the effects of cloud sides on the retrievals. Finally, Section 6 offers a brief summary and discusses the results' main implications.

2. Observations

This study took advantage of the unprecedented abundance of high-quality, easy-to-use, and freely available cloud products from new Earth Observing System (EOS) satellites. In particular, it used a dataset extracted from the continuous stream of incoming MODIS observations at the Goddard Earth Sciences Data and Information Services Center (GES DISC) MODIS data pool. The dataset includes observations from virtually all daytime granules from the MODIS instruments on both the Terra and Aqua satellites for a one year long period ranging from August 2004 to July 2005. The dataset includes 1 km-resolution Collection 4 MODIS products such as the 11 μm brightness temperature, cloud phase, cloud optical thickness, cloud particle size, and cloud top pressure, as well as geolocation parameters such as latitude, longitude, surface type, and sun-view geometry. To reduce data volume, these parameters were saved only for about

every 14th row in the MODIS images. To help examine the influence of local cloud variability, 11 μm brightness temperature and cloud optical thickness values were also saved for both neighbors of each row. Finally, we note that in order to avoid the effects of uncertainties in cloud detection and in ice crystal scattering phase functions, this study analyzed only liquid phase pixels that were flagged as "high confidence" by the operational MODIS optical thickness retrieval algorithm.

3. Methodology

MODIS is suitable for analyzing the view angle dependence of retrieved cloud parameters because clouds are viewed from nadir direction at the MODIS swath center and from highly oblique directions at the swath edges, with maximum viewing zenith angles exceeding 60°. It is important to note that the oblique views are not aligned with the solar azimuth and represent side scattering at both swath edges: At low solar elevations, observations are typically from 60° and 110° relative azimuths at the two swath edges (Figure 1).

One approach to identifying the influence of 3D effects is to contrast the view angle dependence of optical thicknesses (τ) retrieved for homogeneous and inhomogeneous clouds, for which 3D effects are expected to be weaker and stronger, respectively. Following Várnai and Marshak (2002a), we characterize the degree of inhomogeneity at a given pixel through ΔT, the 11 μm brightness temperature gradient in a direction close to the solar azimuth:

$$\Delta T = \frac{\left| T_f - T_b \right|}{d} \tag{1}$$

where T is brightness temperature, the subscripts f and b identify the neighboring pixels in front and behind our pixel, as viewed from the solar direction, and d is the distance between these two neighboring pixels (d=2 km or, if the solar azimuth is close to diagonal in the MODIS image, $d=\sqrt{2}\cdot 2$ km). We note that using the range of brightness temperatures in a 3 X 3 pixel window for characterizing cloud variability produced nearly identical results to our approach, whereas using τ-variability proved less effective in separating homogeneous and inhomogeneous clouds for the purpose of creating two cloud categories with distinct view angle dependencies, perhaps because optical thickness itself is a product of the plane-parallel approximation.

Using the ΔT values defined in Eq. (1), we separated cloudy pixels that had high-confidence liquid phase τ-retrievals into three equally populous categories based on the degree of local cloud variability. Cloudy pixels over ocean and land were assigned into the most homogeneous category if their ΔT value was less than 0.2 °C/km or 0.5 °C/km, respectively. Cloudy pixels over ocean and land were assigned into the most inhomogeneous category if their ΔT value was greater than 0.9 °C/km or 2.2 °C/km, respectively. In summary:

For ocean:

Homogeneous: $\Delta T < 0.2$ °C/km

Intermediate: 0.2 °C/km $\leq \Delta T < 0.9$ °C/km

Inhomogeneous: $\Delta T \geq 0.9$ °C/km

For land:

Homogeneous: $\Delta T < 0.5$ °C/km

Intermediate: 0.5 °C/km $\leq \Delta T < 2.2$ °C/km

Inhomogeneous: $\Delta T \geq 2.2$ °C/km

Local temperature gradients are higher over land than over ocean probably because stronger surface heating causes stronger convection over land. Finally, we note that in plots that do not separate clouds over land and ocean, we combine the two categories by weighting them according to the number of pixels they contain.

4. Results

Considering a variety of solar zenith angles (θ_0), Figure 2 shows the way the mean retrieved τ-values change with view angle (θ) for the most homogeneous and most inhomogeneous third of cloudy pixels. The figure clearly confirms the findings of Loeb and Davies (1996) and Loeb and Coakley (1998) in that 3D effects cause the retrieved τ-values to increase with solar zenith angle. It also shows that homogeneous clouds tend to be thicker than inhomogeneous clouds. In addition, Panel a indicates that for homogeneous clouds, the plane-parallel approximation produces consistent results that don't change much with view direction—although both homogeneous and inhomogeneous clouds tend to be slightly thicker at the more forward scattering swath edge than at the opposite edge. While we have not examined the reasons for this slight cross-track trend, it appears possible that the trend reflects true changes in cloud properties, which could arise from a combination of systematic cross-track variations in local time and latitude (due to the sun-synchronous orbits of the Terra and Aqua satellites) on one hand, and the latitudinal distribution of cloud properties and the daily cycle of cloud development on the other. Panel b, however, reveals that for

inhomogeneous clouds, the plane-parallel approximation yields substantially higher τ-values for oblique views than for overhead views if the sun is fairly oblique. Note that for the most oblique solar zenith angles, the difference exceeds 50%.

Figure 3 shows that clouds tend to be thicker over land than over ocean, and also that the U-shape for inhomogeneous clouds is more pronounced over land than over ocean. This is consistent with the ΔT local temperature gradients being larger over land than over ocean, perhaps because stronger surface heating causes stronger convection over land. This tendency, however, differs from the results of Oreopoulos and Cahalan (2005), who found that large-scale variability over 1° by 1° areas tends to be stronger over ocean. The opposite tendencies at small and large scales indicate that while cloud fields tend to be bumpier over land than over ocean, their statistical properties vary more gradually over land.

Figure 4 illustrates the way the depth of the U-shape changes with solar zenith angle for clouds over land and ocean. The figure characterizes the depth of the U-shape through the $c(\theta_0)$ coefficient obtained by fitting to the mean optical thicknesses in 5°-wide θ_0 intervals a second order polynomial in the form of:

$$\tilde{\tau}(\theta,\theta_0) = a(\theta_0) + b(\theta_0)\cdot\theta + c(\theta_0)\cdot\theta^2 \quad . \tag{2}$$

Figure 5 indicates that the U-shape is stronger for high water clouds, which tend to have larger variability than low clouds. This is consistent with high clouds being thicker both optically and geometrically, which allows more pronounced inhomogeneities. Figure 6 shows that the difference between optical thicknesses retrieved at overhead and oblique views is significant throughout the entire range of cloud thicknesses: for oblique observations, optical thicknesses smaller and larger than 11 are

less and more frequent, respectively. Finally, the results (not shown) indicate that the U-shape is similar over the Northern and Southern hemispheres, for the Terra and Aqua satellites, and for various seasons throughout the year. This allows us to conclude that the presence of the U-shape is not restricted to a particular cloud type or location, but represents the general behavior of MODIS retrievals for inhomogeneous clouds.

5. Potential reasons for the observed behaviors

This section examines the following potential explanations for the U-shape in Figure 3:

- whether inhomogeneous clouds viewed obliquely are indeed thicker than those viewed from overhead,
- whether inhomogeneous clouds behave differently than homogeneous clouds because of their different altitude,
- whether uncertainties in surface reflection, cloud phase, or cloud altitude may cause the behaviors in Figure 3,
- whether cross-track changes in MODIS pixel size may explain the observations,
- whether horizontal photon transport in bumpy clouds may cause the U-shapes in Figure 3,
- and finally, whether the viewing of cloud sides may cause the U-shapes.

We first examine whether the U-shape in Figure 3 may reflect the true behavior of inhomogeneous clouds. It appears unlikely that cross-track variations in local time or latitude—combined with the latitudinal distribution of cloud properties and the daily

cycle of cloud development—could cause the U-shapes observed for inhomogeneous clouds, because the curves remain very similar for various combinations of satellite, hemisphere, and season, even though the local times and latitudes of observations are quite different for the various combinations. Thus it is more likely that the U-shapes do not reflect the true behavior of inhomogeneous clouds, but are caused by some artifact in the retrievals instead.

The next question to consider is whether the difference between the behaviors of homogeneous and inhomogeneous clouds is caused by inhomogeneity itself or by some other difference between the populations of homogeneous and inhomogeneous clouds. Figures 3 and 5 imply that the U-shapes do not arise from inhomogeneous clouds occurring over different surfaces or at different altitudes than homogeneous clouds. Another possibility is that if, due to different updraft speeds, ice crystals had different shapes in homogeneous and inhomogeneous clouds, or if cloud inhomogeneity made it more difficult to detect cloud phase accurately, ice contamination in our supposedly liquid cloud dataset could cause different view-angle dependencies for homogeneous and inhomogeneous clouds. However, this is also unlikely since, as shown in Figure 7, the U-shape is present even if only warm pixels with brightness temperatures exceeding 0°C are considered.

As a result of the considerations above, it appears very likely that the U-shapes in Figure 3 are indeed caused by cloud inhomogeneity. One potential mechanism for this would be if cloud top pressure retrievals were influenced by cloud variability over the operational retrievals' 5 km by 5 km domain, and this caused errors in atmospheric correction over inhomogeneous clouds. Because absorption by tropospheric gases is

negligible at visible MODIS wavelengths, the effects would be strongest in the correction for Rayleigh scattering. However, simple 1D calculations indicate that errors in cloud altitude could cause much weaker effects than those observed, and the changes would have opposite sign at the two sides of MODIS swaths—which is inconsistent with the observations always indicating higher-than-nadir values for oblique views.

Increases in MODIS pixel size for oblique views can also influence the view-angle dependence of retrieved optical thicknesses, because averaging of radiances over larger areas cause stronger plane-parallel biases (e.g., Oreopoulos and Davies 1998). Because of the concavity of the 1D reflectance vs. τ curve, however, averaging always decreases the retrieved τ-values, and so stronger averaging at oblique views would create a $\cap$ shape rather than the U-shape observed in Figure 3.

Theoretical simulations (e.g., Davies 1984, Bréon 1992, Kobayashi 1993) indicate that horizontal photon transport can result in larger optical thicknesses being retrieved for the oblique views typical of MODIS observation geometry than for overhead views, but it is unclear whether this tendency would disappear for high sun. 3D effects could also cause the enhancement at oblique views in Figure 3 by increasing the variability of the reflectance field: Because of the nonlinearity of the 1D reflectance vs. τ curve, retrieved τ-values change more if 3D effects increase, rather than decrease reflectance by a certain amount. As a result, retrieved τ-values can increase more on sunlit slopes than they decrease in shadowy slopes, and this can increase the average τ-value even if 3D effects did not increase the average reflectance. While this behavior has been reproduced in our 3D Monte Carlo simulations, the increase for oblique views occurred exclusively at pixels whose brightness was enhanced by 3D effects. This, however, does not seem to fit

the observations in which the U-shape appears even for pixels for which $T_f < T_b$, which tend to lie on slopes facing away from the sun and to be darkened by 3D effects (Fig. 8).

Finally, cloud side viewing also influences the view angle dependence of retrieved τ-values. The observations of Minnis (1989) indicate that cloud side viewing must occur quite frequently indeed, because it significantly increases cloud coverage for oblique views. Reflection into oblique directions is generally enhanced through cloud sides, including sides of thicker cloud elements that are surrounded by significantly thinner regions. Cloud side viewing can also cause the U-shape in Figure 3 because while overhead views can see through small subpixel gaps in cloudiness, oblique views tend to see cloud sides instead. This can result in stronger plane-parallel biases and thus stronger reductions in retrieved optical thicknesses for overhead views than for oblique views. While such side-viewing occurs for any solar elevation, its effects are stronger for oblique sun because of the more pronounced the nonlinearity (i.e., earlier saturation) of the 1D reflectance vs. τ curve. Still, we are somewhat cautioned by the U-shape being present even for pixels that are surrounded by cloudy pixels on all sides and are farther than 10 km away from clear pixels in cross-track direction (Figure 9). This observation, however, doesn't exclude side viewing from being an important factor in creating the U-shape in Figure 3, because subpixel gaps can occur in areas that appear overcast at 1 km resolution, and also because side viewing can have important effects in multilayer cloud systems or even in highly variable clouds.

6. Summary and discussion

This paper examined whether cloud inhomogeneity introduces any view angle dependent biases into MODIS cloud optical thickness (τ) retrievals, which use the plane-parallel approximation and hence assume cloud homogeneity. The influence of cloud inhomogeneity was identified by contrasting the view angle dependence of mean τ values retrieved for clouds that were deemed homogeneous or inhomogeneous based on the local gradient in 11 μm brightness temperature.

The analysis of liquid phase clouds in a one year-long global dataset of Collection 4 MODIS cloud products revealed that while optical thickness retrievals give remarkably consistent results at all view directions for homogeneous clouds, they give systematically higher τ-values at oblique views than at overhead views for inhomogeneous clouds if the sun is fairly oblique. The mean optical thickness retrieved for the most inhomogeneous third of cloudy pixels is more than 30% higher for oblique views at swath edges than for overhead views at the swath center if the solar zenith angle is 60°; the difference exceeds 40% if the solar zenith angle is 70°. The observations reveal that the dependence on view angle is stronger for higher clouds and for clouds over land, that it is present over a wide range of cloud thicknesses at both hemispheres through all seasons, and that it is quite similar in observations by the Terra and Aqua satellites.

After considering several potential scenarios, the paper concluded that the observed behavior is indeed caused by cloud inhomogeneities influencing 1D cloud property retrievals, and not by other differences between homogeneous and

inhomogeneous clouds that are unrelated to inhomogeneity itself (e.g., in microphysics). The paper discussed several mechanisms through which cloud inhomogeneity may influence the view angle dependence of τ-values. The most likely candidate is the increased viewing of cloud sides from oblique directions. Cloud sides can enhance reflection into oblique directions, and while cloudy pixels may contain small gaps among broken clouds in overhead views, these dark gaps tend to be filled by cloud sides in oblique views.

Once the dominant mechanism is identified unambiguously, it will be possible to determine whether the view angle dependent biases decrease τ-values for nadir views or increase them for oblique views. We note, however, that the view angle dependent biases discussed in this paper are only one component of the overall radiative effect of cloud inhomogeneity which, as discussed in earlier studies (Loeb and Davies 1996; Loeb and Coakley 1998), increases τ with solar zenith angle even for overhead views—though by not as much as for oblique views.

The results presented here can help improve future versions of the τ-retrieval uncertainty estimates that will start accompanying MODIS cloud products in Collection 5. These uncertainty estimates consider only factors within a 1D framework (such as uncertainties in calibration, in atmospheric correction, and in surface albedo), whereas our results suggest that identifying inhomogeneous pixels through local brightness temperature gradients could help incorporating view angle dependent cloud inhomogeneity effects as well—and this approach may eventually help correct for the observed view angle dependent biases.

Acknowledgments

We are grateful to Eunice Eng for her help in extracting our dataset from the MODIS data pool. This research was supported by the NASA Radiation Sciences Program under grants 621-30-86 and 622-42-57.

References

Ackerman, S. A., K. I. Strabala, W. P. Menzel, R. A. Frey, C. C. Moeller, and L. E. Grumley, 1998: Discriminating clear sky form clouds with MODIS. *J. Geophys. Res.*, **103**, 32,141-32,158.

Bréon, F.-M., 1992: Reflectance of broken cloud fields: Simulation and parameterization. *J. Atmos. Sci.*, **49**, 1221-1232.

Buriez, J.-C., M. Doutriaux-Boucher, F. Parol, and N. G. Loeb, 2001: Angular variability of the liquid water cloud optical thickness retrieved from ADEOS-POLDER. *J. Atmos. Sci.*, **58**, 3007-3018.

Chambers, L. H., B. A. Wielicki, and N. G. Loeb, 2001: Shortwave flux from satellite-measured radiance: A theoretical study over marine boundary layer clouds. *J. Appl. Meteor.*, **40**, 2144-2161.

Cornet, C., H. Isaka, B. Guillemet, and F. Szczap, 2004 : Neural network retrieval of cloud parameters of inhomogeneous clouds from multispectral and multiscale radiance data: Feasibility study. *J. Geophys. Res.*, **109**, D12203, DOI 10.1029/2003JD004186.

Cornet, C., J.-C. Buriez, J. Riédi, H. Isaka, B. Guillemet, 2005: Case study of inhomogeneous cloud parameter retrieval from MODIS data, *Geophys. Res. Lett.*, **32**, L13807, doi:10.1029/2005GL022791.

Davies, R., 1984: Reflected solar radiances from broken cloud scenes and the interpretation of scanner measurements. *J. Geophys. Res.*, **89**, 1259-1266.

Davis, A., A. Marshak, R. F. Cahalan, and W. J. Wiscombe, 1997: The Landsat scale break in stratocumulus as a three-dimensional radiative transfer effect, Implications for cloud remote sensing. *J Atmos. Sci.*, **54**, 241-260.

Faure, T., H. Isaka, and B. Guillemet, 2001: Neural network retrieval of cloud parameters of inhomogeneous and fractional clouds. Feasibility study. *Remote Sens. Environ.*, **77**, 123-138.

Horváth, Á., and R. Davies, 2004: Anisotropy of water cloud reflectance: A comparison of measurements and 1D theory. *Geophys. Res. Lett.*, **31**, L01102, doi: 10.1029/2003GL018386.

Iwabuchi, H., and T. Hayasaka, 2002: Effects of cloud horizontal inhomogeneity on the optical thickness retrieved from moderate-resolution satellite data. *J. Atmos. Sci.*, **59**, 2227–2242.

Iwabuchi, H., and T. Hayasaka, 2003: A multi-spectral non-local method for retrieval of boundary layer cloud properties from optical remote sensing data. *Remote Sens. Environ.*, **88**, 294-308.

Kobayashi, T., 1993: Effects due to cloud geometry on biases in the albedo derived from radiance measurements. *J. Climate*, **6**, 120-128.

Loeb, N. G., and R. Davies, 1996: Observational evidence of plane-parallel model biases: Apparent dependence of cloud optical depth on solar zenith angle. *J. Geophys. Res.*, **101**, 1621-1634.

Loeb, N. G., and R. Davies, 1997: Angular dependence of observed reflectances: A comparison with plane-parallel theory. *J. Geophys. Res.*, **102**, 6865-6881.

Loeb, N. G., and J. A. Coakley, 1998: Inference of marine stratus cloud optical depths from satellite measurements: Does 1D theory apply? *J. Climate*, **11**, 215-233.

Loeb, N. G., T. Várnai, and R. Davies, 1997: Effect of cloud inhomogeneities on the solar zenith angle dependence of nadir reflectance. *J. Geophys. Res.*, **102**, 9387-9395.

Loeb, N. G., T. Várnai, D. M. Winker, 1998: Influence of subpixel-scale cloud-rop structure on reflectances from overcast stratiform cloud layers. *J. Atmos. Sci.*, **55**, 2960-2973.

Marchand, R., and T. Ackerman, 2004: Evaluation of radiometric measurements from the NASA Multiangle Imaging Spectroradiometer (MISR): Two- and three-dimensional radiative transfer modeling of an inhomogeneous stratocumulus cloud deck. 109 (D18), D18208, doi:10.1029/2004JD004710.

Marshak, A., A. Davis, W. J. Wiscombe, and R. F. Cahalan, 1995: Radiative smoothing in fractal clouds. *J. Geophys. Res.*, **100**, 26247-26261.

Marshak, A., A, Davis, R. F. Cahalan, and W. Wiscombe, 1998: Nonlocal independent pixel approximation: Direct and inverse problems. *IEEE Trans. Geosci.*, **36**, 192-205.

Minnis, P., 1989: Viewing zenith angle dependence of cloudiness determined from coincident GOES East and GOES West data. *J. Geophys. Res.*, **94**, 2303-2320.

Oreopoulos, L., and R. Davies, 1998: Plane Parallel Albedo Biases from Satellite Observations. Part I: Dependence on Resolution and Other Factors. *J. Climate*, **11**, 919–932.

Oreopoulos, L., and R. F. Cahalan, 2005: Cloud inhomogeneity from MODIS. *J. Climate.* (In press)

Oreopoulos, L., R. F. Cahalan, A. Marshak, and G. Wen, 2000: A new normalized difference cloud retrieval technique applied to Landsat radiances over the Oklahoma ARM site. *J. Appl. Meteor.*, **39**, 2305-2321.

Oreopoulos, L., A. Marshak, R. F. Cahalan, and G. Wen, 2000: Cloud 3D effects evidenced in Landsat spatial power spectra and autocorrelation functions. *J. Geophys. Res.*, **105**, 14777-14788.

Platnick, S., M. D. King, S. A. Ackerman, W. P. Menzel, B. A. Baum, J. C. Riédi, and R. A. Frey, 2003: The MODIS cloud products: Algorithms and examples from Terra. *IEEE Trans. Geosci. Remote Sens.*, **41**, 459-473.

Rossow, W., 1989: Measuring cloud properties from space: A review. *J. Climate*, **2**, 201-213.

Stamnes, K., S.-C. Tsay, W. J. Wiscombe and K. Jayaweera, 1988: Numerically stable algorithm for discrete-ordinate-method radiative transfer in multiple scattering and emitting layered media. *Appl. Opt.*, **27**, 2502–2512.

Szczap, F., H. Isaka, M. Saute, B. Guillemet, and Yahya Gour, 2000: Inhomogeneity effects of 1D and 2D bounded cascade model clouds on their effective radiative properties, *Phys. Chem. Earth*, **25**, 83-89.

Várnai, T., 2000: Influence of three-dimensional radiative effects on the spatial distribution of shortwave cloud reflection. *J. Atmos. Sci.*, **57**, 216-229.

Várnai, T., and A. Marshak, 2002a: Observations of three-dimensional radiative effects that influence MODIS cloud optical thickness retrievals. *J. Atmos. Sci.*, **59**, 1607-1618.

Várnai, T., and A. Marshak, 2002b: Observations of three-dimensional radiative effects that influence satellite retrievals of cloud properties. *Quart. J. of Hungarian Meteor. Service* (*Időjárás*), **106**, 265-278.

Yang, P., and K. N. Liou, 1996: Finite-difference time domain method for light scattering by small ice crystals in three-dimensional space, *J. Opt. Soc. Am.*, **10**, 2072-2085.

Zuidema, P., R. Davies, and C. Moroney, 2003: On the angular radiance closure of tropical cumulus congestus clouds observed by MISR. *J. Geophys. Res.*, **108**, No. D20, 4626, doi: 10.1029/2003JD003401.

Figures

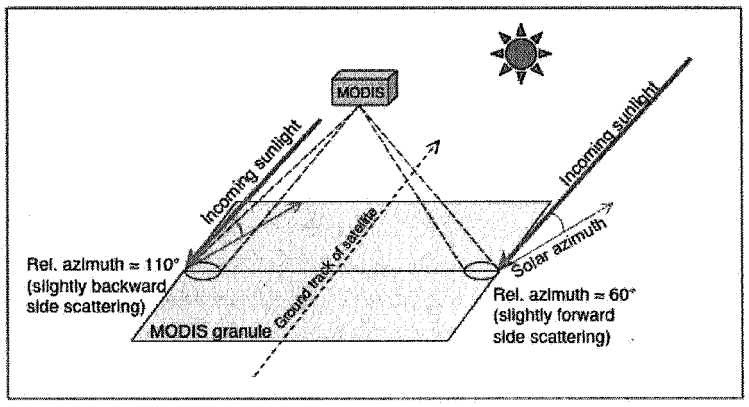

Figure 1. Schematic view of MODIS observational geometry.

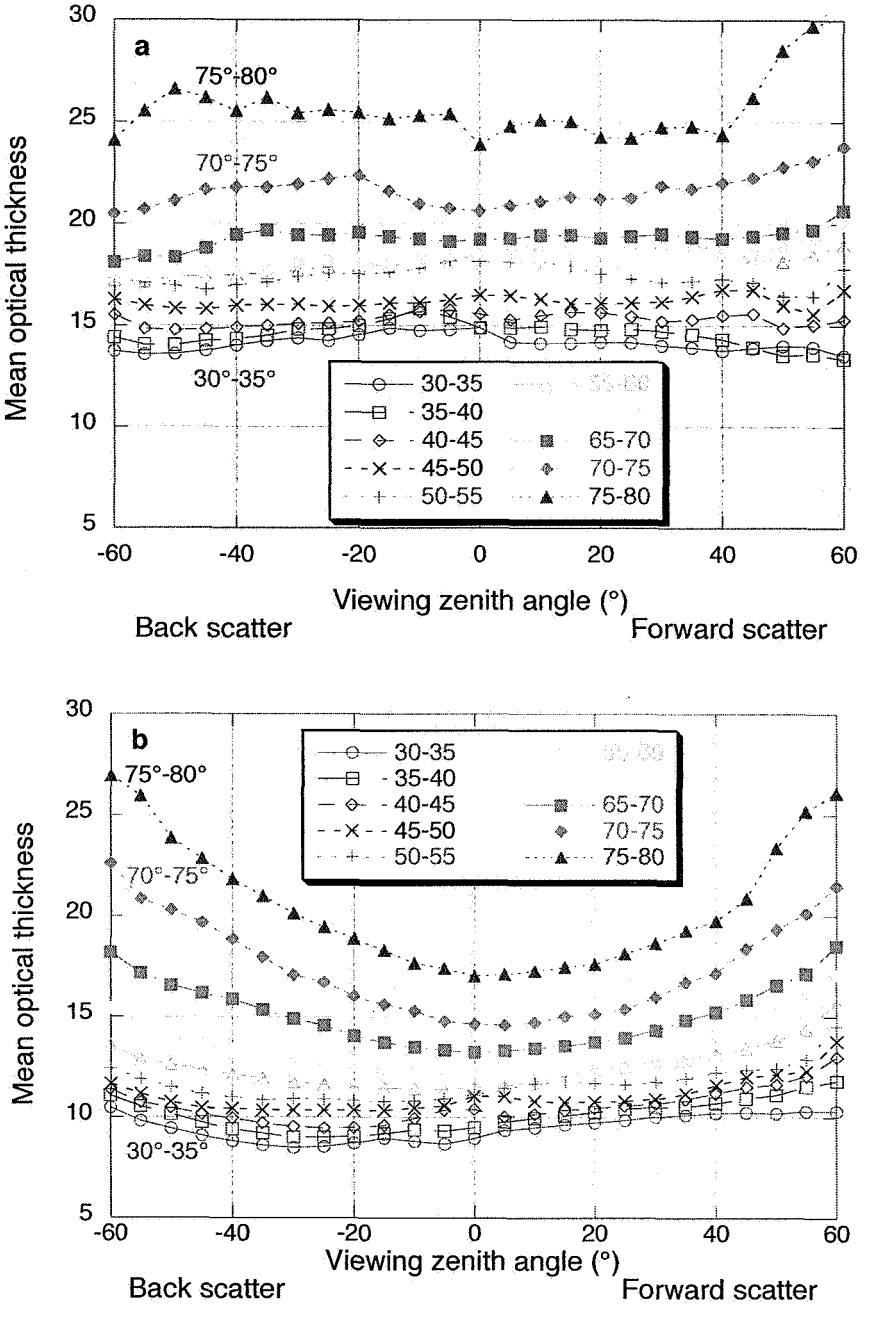

Figure 2. View angle-dependence of mean retrieved optical thickness. Only liquid phase clouds with high-confidence retrievals are considered. Each line represents a separate solar zenith angle (θ_0) interval. (a) Most homogeneous third of cloudy pixels; (b) Most inhomogeneous third of cloudy pixels.

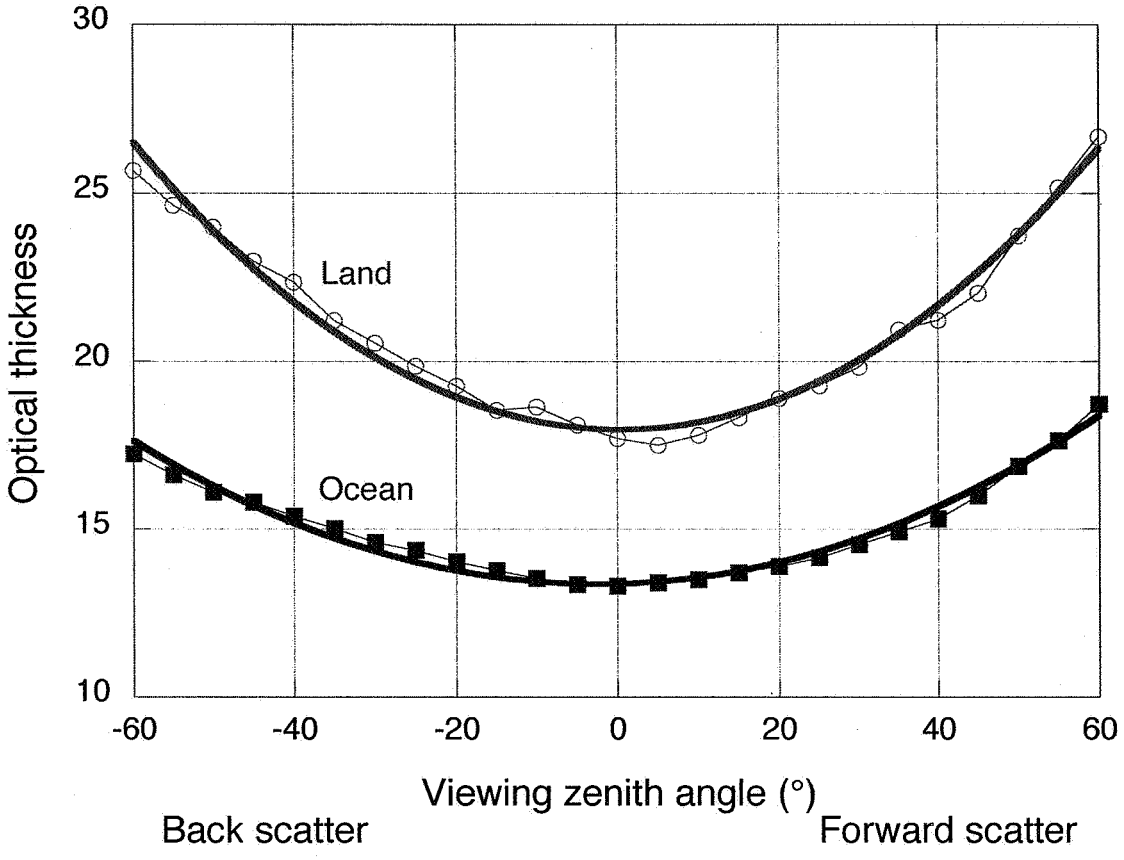

Figure 3. View angle dependence of mean optical thickness of inhomogeneous clouds over land and ocean. For increased clarity, each curve represents the average for 5 different solar zenith angle intervals ranging from 55° to 80°. The thick solid lines represent second-order polynomial fits to the curves.

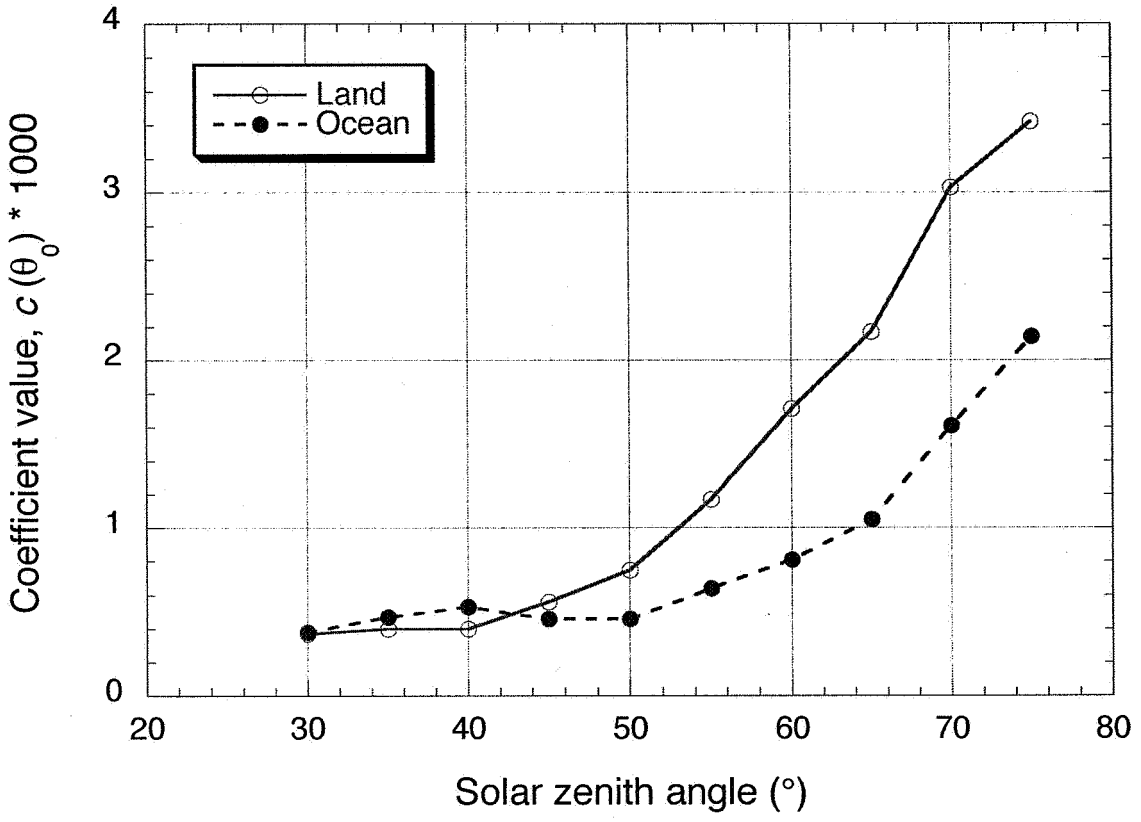

Figure 4. Solar zenith angle dependence of $c(\theta_0)$ quadratic coefficient values that were obtained by fitting second-order polynomial to the view-angle dependence of retrieved τ-values.

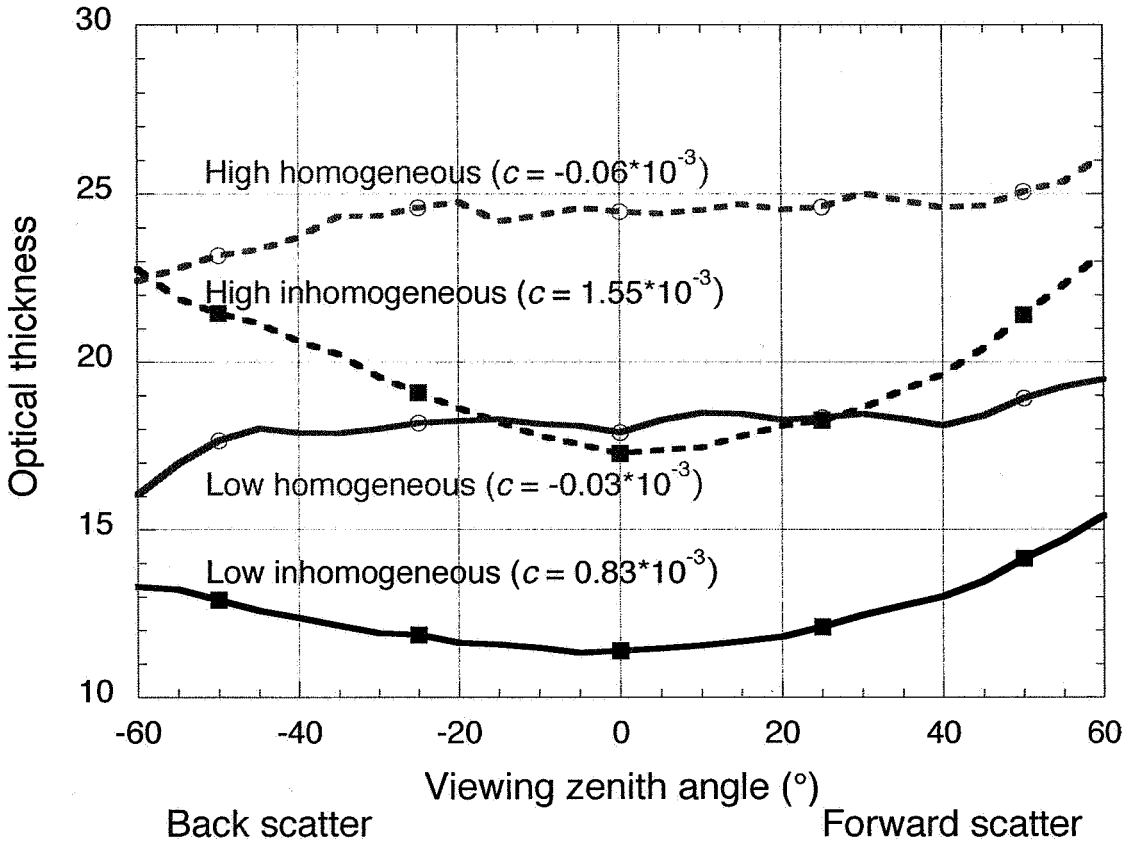

Figure 5. View angle dependence of mean τ for the most homogeneous and most inhomogeneous third of cloudy pixels that have MODIS-estimated cloud top pressures below and above 700 hPa. Accordingly, the "high" and "low" curves represent clouds with tops higher and lower than about 3 km, respectively. For increased clarity, each curve represents the average for 5 different solar zenith angle intervals ranging from 55° to 80°. The figure also displays the c coefficients obtained by fitting a second-order polynomial to each curve.

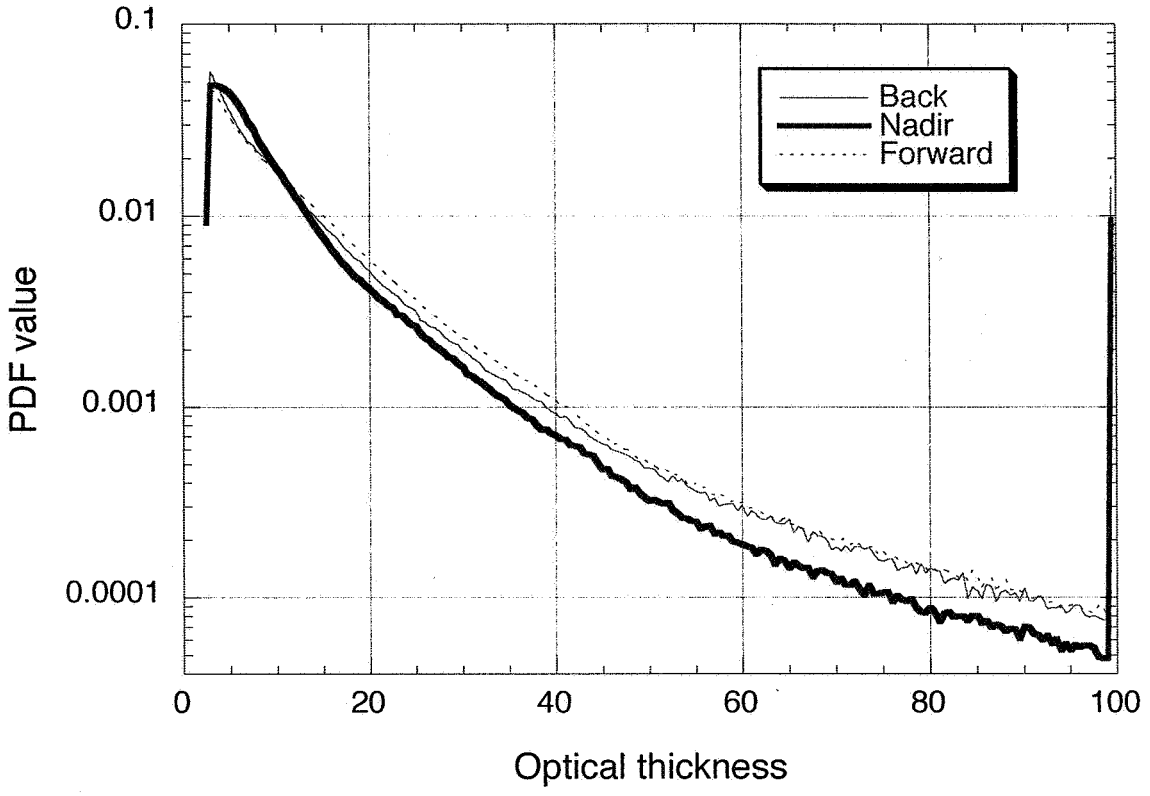

Figure 6. Probability distribution function (PDF) of τ for the most inhomogeneous third of cloudy pixels for nadir view and for oblique views slightly oriented toward forward and back scatter. The viewing zenith angle is in the 50°-60° and the 0°-5° range, respectively; the solar zenith angle is between 60° and 70°.

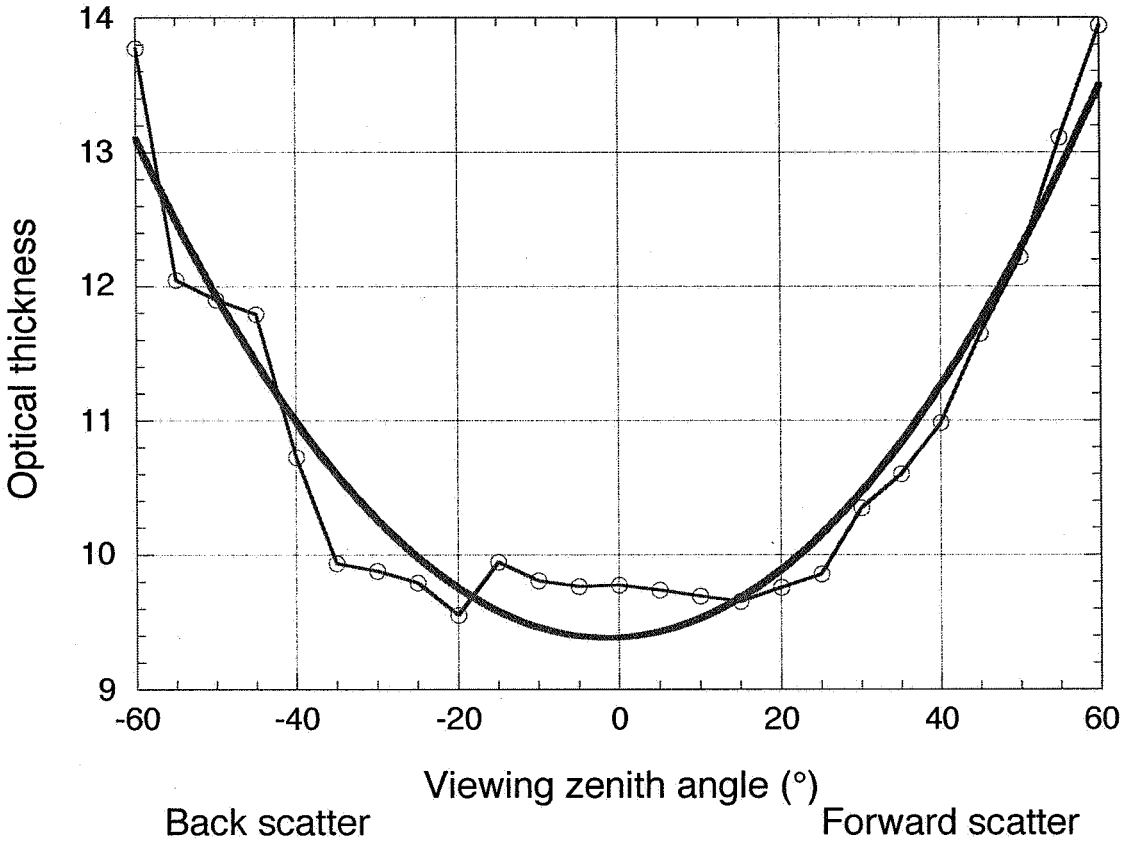

Figure 7. View angle dependence of mean τ for inhomogeneous pixels with 11 μm brightness temperatures warmer than 0°C, for solar zenith angle ranging from 55° to 80°. The thick line represents a second order polynomial fit to the data, with c= 1.0*10^{-3}.

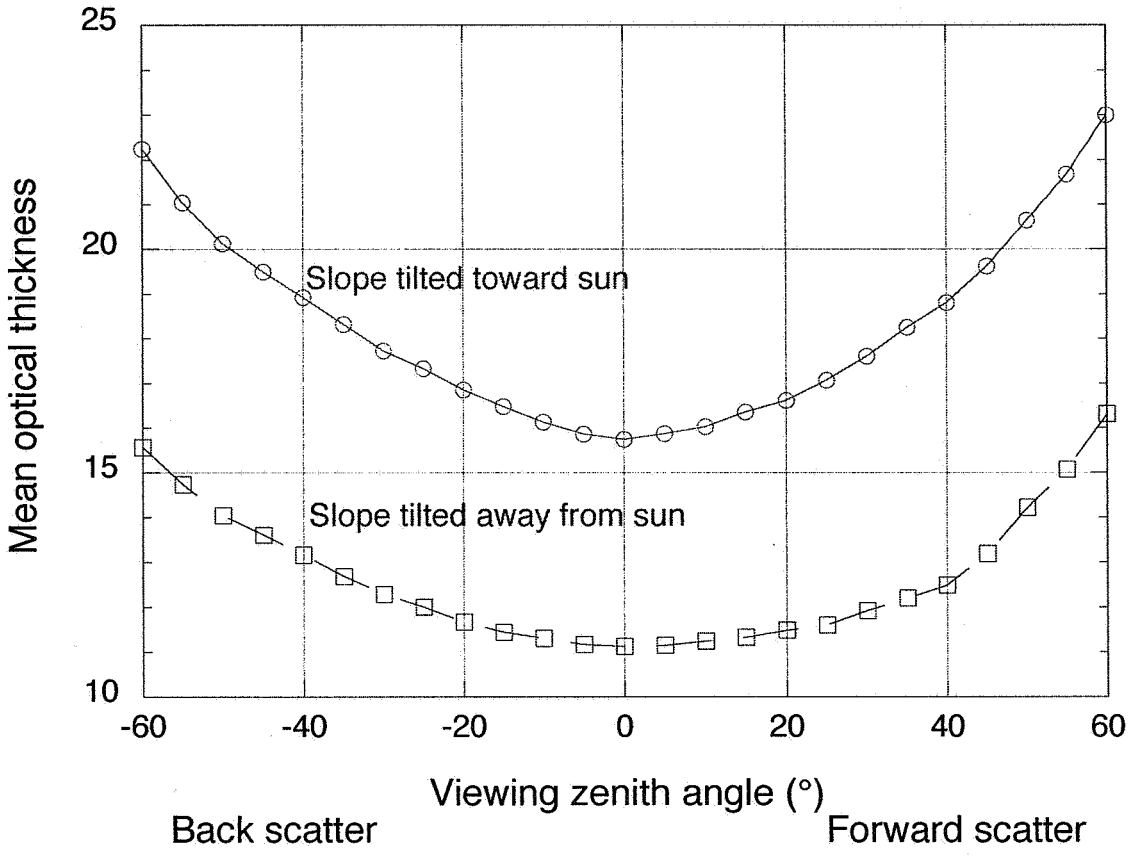

Figure 8. View angle dependence of τ for inhomogeneous pixels that lie on slopes tilted toward and away from the sun ($T_f > T_b$ and $T_f < T_b$, respectively). The curves represent the average for 5 different solar zenith angle intervals ranging from 55° to 80°. The quadratic polynomial coefficients for slopes tilted toward and away from the sun are c=1.82*10^{-3} and 1.28*10^{-3}, respectively.

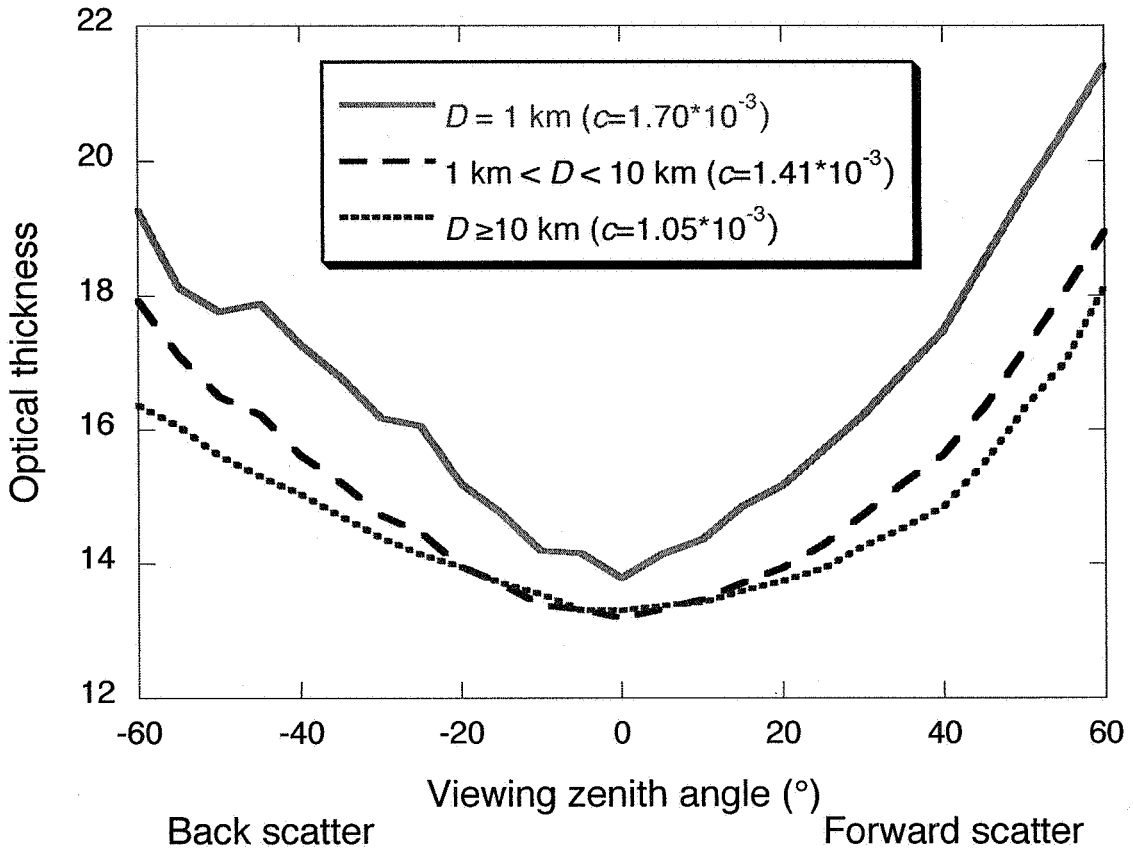

Figure 9. View angle dependence of mean optical thickness for inhomogeneous pixels that occur at various distances *D* from the nearest cloud-free pixel in cross-track direction. The curves represent the average for 5 different solar zenith angle intervals ranging from 55° to 80°. Values of quadratic polynomial coefficient *c* are also displayed.